Optical and Quantum Electronics **33:** 527–540, 2001.

All-optical security coded key

F. GARZIA* AND M. BERTOLOTTI
*INFM Dipartimento di Energetica, Università degli Studi di Roma "La Sapienza", Via A. Scarpa 14, 00161 Rome, Italy (*author for correspondence: E-mail: fabio.garzia@uniroma1.it)*

Abstract. We present a device that is able to generate a coded sequence of pulses using a proper sequence of input pulses. It behaves as a security coded key that does not need external energy to work.

Key words: all-optical device, all-optical switching, security device, soliton interaction

1. Introduction

The interesting effects of soliton propagation at the interface between two nonlinear materials (Aceves *et al.* 1988; Varatharajah *et al.* 1989; Aceves *et al.* 1990) or in a material in the presence of a gaussian refractive index profile, that is in low perturbation regime (Garzia *et al.* 1997, 1998) demonstrate that it is possible to switch a soliton, in the presence of a transverse refractive index variation, towards a fixed path, since the index variation acts as a perturbation against which the soliton reacts as a particle, moving as a packet without any loss of energy.

In particular it is possible to select the intensity level that a soliton beam must have to be trapped inside a curved waveguide (Garzia *et al.* 1999) and to be propagated to a certain position, and the relative acceleration between two solitons when they interact due to their partial overlapping (Garzia *et al.* 2000).

In this paper we use the two mentioned properties to design an all-optical device that acts as a security coded key that is capable of emitting a proper pulsed code, that can be hundred of bits long, once it has been properly queried by an input sequence of pulses.

In our geometry a soliton beam travels in a waveguide which, in the plane between the cladding and the substrate, has a distribution of refractive index which follows a triangular curve, with a longitudinal parabolic profile, whose properties have been already described (Garzia *et al.* 1998, 1999, 2000).

We first illustrate the general structure of the device then we design the proposed device and then we test it by means of numerical simulations. Further we discuss some points concerning the limits for the correct working of the security key.

2. Structure of the security key

The device is composed by N equal elementary looped cells, where N is the number of pulses that compose the code, whose maximum number is limited by the absorption of the device.

A stream of N pulses is used to query the key to emit its pulsed code. In the following we will also use the term bit to indicate the binary information carried by the presence or the absence of a particular pulse. In Fig. 1 a two bit key is shown. The first pulse enters the device and it is attracted by the outer loop whose structure is studied to give to the soliton pulse, after a round trip inside it, a repulsive relative phase when it interacts with the following pulses of the querying code. Thanks to this property, the subsequent pulses are repulsed and kept on the main waveguide reaching the following stages of the device, where the process repeats again, while the soliton pulse propagates in the inner loop.

Once all the querying pulses have entered the key, the first pulse, that has propagated inside the first loop, is no more kept inside it by the relative repulsion with the other pulses and exit the loop, propagating transversally

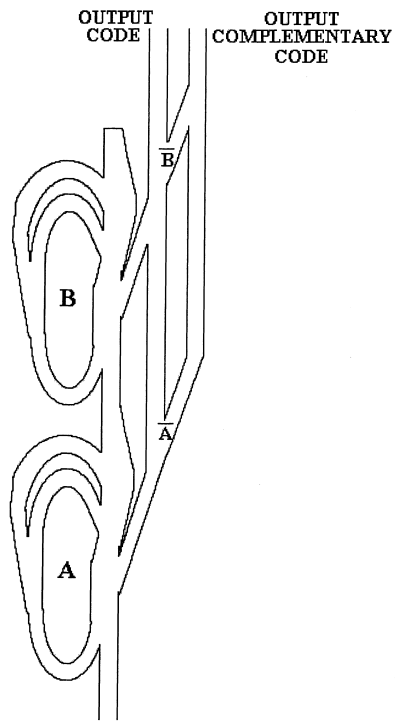

Fig. 1. Scheme of a two bit security key. $\bar{A}$ and $\bar{B}$ represent the code selection junctions of pulses related to the loops A and B respectively.

and reaching the output code waveguide where it can remain, if it belongs to the code, or it can cross it, reaching the output complementary code waveguide if it does not belong to the code, according to the proper designed propagation properties of the $\bar{A}$ junction.

The selection of the code can be made by means of the opening or the closing of the transversal waveguides that can be constituted by Y-junctions or analogous structures, whose behaviour is well-known and that are not studied here for brevity. These transversal waveguides connect the output code waveguide with the output complementary code waveguide and they can be opened or closed from the point of view of the propagation of the soliton beams. The particular design of the device allows the use of a common basic structure for all the keys while the code of each key is programmed by means of simple operations of opening or closing of the transversal waveguides performed during the production phase or in a second time.

The expulsion process from the loops takes place according to a sequence that is equal to the input sequence of the querying pulses that direct themselves towards the output code waveguide where they are selected as belonging to the code or to the complementary code.

Also the last pulse of the querying sequence needs to propagate in a loop to respect the temporal relation with the other pulses, even if it does not switch any further pulse.

We want now to describe into details the structure of the elementary loop cell that composes the device, the scheme which is shown in Fig. 2. Since it is necessary to change the relative phase of the pulse that propagates inside the loop only once, to make it repel with the following pulses, a double branched

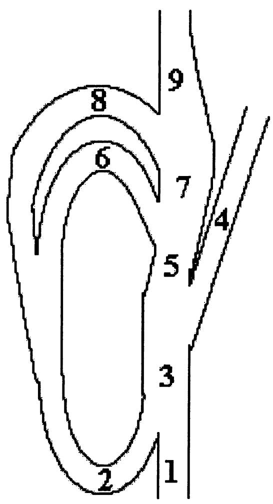

Fig. 2. Scheme of an elementary loop cell.

loop is used. The first pulse enters the waveguide 1 and propagates through the waveguide 3, passing over the input of the waveguide 4 and the branch 6 of the loop, since they are both characterised by the same refractive index of the main waveguide and therefore the pulse is not attracted inside them. Since branch 8 of the loop is characterised by a higher refractive index, the pulse is instead captured inside it. The length of this branch is calculated so that the pulse experiences a phase variation that makes the soliton to repel the following pulses.

The soliton pulse propagates inside the loop until reaching again the point 3 where it propagates parallel with respect to the following pulse and slightly overlapped with it so that the mutual repulsive force does not allow the first pulse to enter the output waveguide 4.

The two pulses reach therefore the point 5 where the waveguide becomes narrower and the mutual repulsive force greatly increases, pushing the first pulse into the branch 6 of the loop and the second pulse towards the right hand side of the point 7 of the waveguide that becomes wider. In this situation the second pulse is far enough from the branch 8 of the loop to be attracted inside it, and it can reach the point 9 of the waveguide where it exits, reaching the following stage.

The first pulse propagates now into the shorter loop 6, whose length is calculated to let it have the same repulsive phase with respect to the other pulses after each trip, repeating the same process.

When all the querying pulses have entered the device the first pulse reach the point 3 where it does not find any repulsive action owed to the presence of the following pulse and it moves transversally until reaching the waveguide 4 that takes it in the output code waveguide where it is selected as belonging to the code or to the complementary code, according to the mechanism we have discussed.

We briefly illustrate now the profile of the refractive index of the waveguides, the properties of the longitudinal parabolic waveguides that composes the loop and the interaction force between solitons necessary to design the device.

3. Properties of a soliton in a longitudinal parabolic waveguide

The loop structure is composed by longitudinal parabolic paths whose transverse refractive index profile follows a triangular distribution (Garzia *et al.* 1998). We choose this kind of waveguide because it is the simplest curve that takes progressively the soliton beam to the interaction point of the waveguides and then again into the loop. Further the parabolic path is the trajectory followed from a soliton beam that is injected into a triangular transverse refractive index profile, that is the transverse profile that we are going to consider (Garzia *et al.* 1999). The local inclination of this longitudinally parabolic waveguide with respect to the longitudinal axes increases with propagation distance: this means that it is necessary to impose some limits to avoid of overcoming the paraxial approximation, endangering the validity of the nonlinear Schroedinger equation (NLSE) and therefore of the whole theory we are developing. For this reason two mirrors are used to close the loop (Garzia *et al.* 1999, 2000).

A soliton beam propagating in the z-direction, is characterised by the following expression of the field Q at the beginning of the structure:

$$Q(x,0) = C\,\mathrm{sech}[C(x-\bar{x})], \tag{1}$$

where $\bar{x}$ is the position of the centre of the beam and C is a real constant from which both the width and the amplitude of the field depend. The variables x and z are normalised with respect to the wavevector of the wave and therefore they are not dimensional.

When the soliton beam is propagating in a triangular transverse index profile, whose maximum value is Δn_0 and whose maximum width is $2b$, it is subjected to a transverse acceleration (Chen and Liu 1978; Cow 1982; Garzia *et al.* 1998). If $x_G(z)$ is the position of the central part of the waveguide profile with respect to z, the longitudinal expression of the waveguide chosen to be parabolic is characterised by the following expression:

$$x_G(z) = az^2, \tag{2}$$

where 'a' is a real constant responsible for the local inclination of the waveguide with respect to the longitudinal axis.

In this situation it is possible to demonstrate that the beam remains trapped inside this waveguide if its amplitude is greater than:

$$C_D = \left(\frac{ab}{\Delta n_0}\right)^{1/2}. \tag{3}$$

If $C \to 0$, it is necessary to act on the parameters of Equation (3) to reduce C_D and to lock-in the beam inside the waveguide. This can be done increasing the refractive index Δn_0 or reducing the parameters b and 'a'.

The refractive index Δn_0 can't overcome a certain level to avoid the generation of strong index gradient that would disturb the phenomena involved. There are anyway some physical limitations in the realisations of high refractive index profiles.

The parameter b can be reduced until reaching the width of the beam profile under which the index profile does not act uniformly on the trapped beam.

The parameter 'a' is responsible for the local inclination of the longitudinal parabolic waveguide: the lower its value the greater the linearity of the curve. This means that it is anyway possible to guide the soliton beams using linear waveguides (Garzia *et al.* 1998) without influencing the correct working of the device since the core mechanism is based on the interaction of the solitons that takes place in the merging point between the waveguides. A longitudinally parabolic waveguide is anyway used for the reasons illustrated at the begin of this paragraph.

Since we deal with a parabolic waveguide, we are in the presence of a local inclination, with respect to the z axis, that increases with z. We should not forget that we are in a paraxial approximation, that is the derived equations are valid until the angle between the propagation direction and the longitudinal direction is lesser than 8°–10°. This means that, due to the analytical expression of the waveguide, expressed from Equation (2), once the 'a' parameter has been chosen, the propagation variable z can reach a maximum value over which the paraxial approximation is no more valid. In analytical terms it means that it is possible to impose this condition to the first derivative of Equation (2) to calculate the maximum propagation distance:

$$x'_{\mathrm{G}}(z_{\max}) = \tan 8^\circ = 0.14 = 2az_{\max}, \tag{4}$$

that can be solved respect to $z_{\max}$ giving:

$$z_{\max} = \frac{7 \times 10^{-2}}{a}. \tag{5}$$

Substituting Equation (5) into Equation (2) it is possible to calculate the correspondent $x_{\max}$:

$$x_{\max} = \frac{4.9 \times 10^{-3}}{a}. \tag{6}$$

This means that, once a parabolic profile has been chosen through the 'a' parameter, the soliton can propagate in it for a maximum distance equal to $z_{\max}$. This condition must be considered in the design of the loop waveguide.

For this reason it is not possible to use a closed curve and it is necessary to use two mirrors to close the propagation loop.

4. Interaction acceleration of soliton beams

To let our device work properly we use the interaction force between solitons whose expression has been demonstrated to be an exponential function of the relative distance d and a cosinusoidal function of the relative phase ϕ, according to the following equation (Garzia *et al.* 2000):

$$a(d, \varphi) = \frac{C^2}{5} \exp(-C(d - 2x_{\mathrm{HHHW}})) \cos \phi, \quad (d \geq 2x_{\mathrm{HHHW}}) \tag{7}$$

where x_{HHHW} is the half-height half-width that is the distance from the centre of the beam where the amplitude reduces to one half, equal to:

$$x_{\mathrm{HHHW}} = \frac{1}{C} \log(2 + \sqrt{3}), \tag{8}$$

The expression (7) is very useful in the quantification of the mutual acceleration between solitons and it is used to design the device.

5. Design of the device

We start by designing the parabolic waveguide. We choose for the main loop a refractive index Δn_0 equal to 10^{-3}. If we also choose $b = 1$ and $a = 4 \times 10^{-4}$ we can calculate from Equation (3) the lock-in value for the amplitude that is about 0.4. We decide to use, for our device, a value for the amplitude C equal to 2. Once chosen the main loop, since we are free to decide the temporal length of the pulses, it is necessary to define its maximum length. We have to remember that the paraxial approximation imposes the curve not to exceed a curvature of about 8°–10° with respect to the longitudinal axes.

Substituting $a = 4 \times 10^{-4}$ into Equation (5) we have $z_{\max} = 175$ that substituted into Equation (6) gives $x_{\max} = 12.25$: if we let the curve extend up to a transversal distance equal to 10, that is a longitudinal distance equal to 158, the paraxial approximation is respected.

We have now to define the external half-loop, that is the loop where the beam propagates only the first time to acquire a repulsive relative phase difference with respect to the following pulse of the code. The transversal length of this curve is imposed by the internal curve. The difference between the total length of the external curve and the total length of the internal curve multiplied by two gives the difference of path between the two curves. Since we deal with normalised wavevectors and refractive index, this difference is also equal to the phase difference. Since the phase is periodical, it is possible to choose different values for the '*a*' parameter of the curve, without taking care of the paraxial approximation, that is surely respected since this half-loop is less curved with respect to the internal loop that already respects this condition. The only restriction is represented by the total length of the structure that we want to be as short as possible. The research of this '*a*' value can be made numerically: a repulsive phase difference is attained, for example, if we chose for the external loop $a = 1.99 \times 10^{-4}$. The transversal extension of this curve is equal to 10, since we have imposed this value for analogy with the internal loop, while its longitudinal distance, calculated using Equation (2), is 224, that is obviously a higher value with respect to the internal loop.

We have finally to choose a higher value for the refractive index Δn_0 with respect to the internal loop and to the main waveguide, so that the half-loop is able to attract and capture the soliton beams that propagates close to its entrance. If we chose, for example, $\Delta n_0 = 1.5 \times 10^{-3}$, we attain this effect and it is immediate possible to demonstrate, by means of Equation (3) that the lock-in value for the amplitude for this half-loop is about equal to 0.36, that is 10% less than lock-in value for the internal value. This ensures that, if a soliton beam is trapped inside the internal loop it is surely trapped inside the external loop. Since we have chosen $C = 2$, the beams we are considering are surely trapped by both the loops.

We have designed, until this point, the loop structure of the device. It is now necessary to design the structure of the main waveguide. We chose a bit higher refractive index with respect to the internal loop, that is $\Delta n_0 = 1 \times 10^{-3}$, so that the beams that propagates inside it tend to be expelled towards the main waveguide. The value chosen is $\Delta n_0 = 1.1 \times 10^{-3}$.

The expression of the transversal acceleration of a soliton beam in a linear transversal refractive index profile is equal to (Garzia *et al.* 1998):

$$a_T = \frac{2\Delta n_0}{b} C^2. \tag{9}$$

When the beam propagates from loop 2 to the zone 3 of the waveguide it is subjected to a force that tends to attract it inside the loop and a force that tends to attract it inside the main waveguide, in an opposite direction. Since the refractive index of the main waveguide is a bit higher with respect to the loop, the beam tends to move slowly towards it with an acceleration that can be calculated from Equation (9), where Δn_0 is the difference between the two refractive index. Substituting the numerical values we have $a_T = 8 \times 10^{-4}$. Since the transversal co-ordinate of the beam x_B is related to its longitudinal co-ordinate from:

$$x_B = \tfrac{1}{2} a_T z^2, \tag{10}$$

it is possible to resolve Equation (10) with respect to z giving:

$$z = \sqrt{\frac{2x_B}{a_T}}. \tag{11}$$

Since the transversal distance from one side to the other of the main waveguide is equal to 2, substituting the numerical values into Equation (11) we obtain that $z = 70$, that is the longitudinal distance between the exit of the loop 3 and the entrance of the waveguide 4.

Since the beam is attracted out of the loop from an acceleration equal to $a_T = 8 \times 10^{-4}$, it is possible to determine the relative distance, between two solitons inside the zone 3 of the waveguide, that generates a repulsive force exactly equal to the transverse force generated by the index profile. Using Equation (7) we have $d = 4.4$, that is the maximum distance above which the repulsive force is no more able to balance the attraction force. Using a shorter distance we are sure that not only the attraction force is compensated but that one soliton is also pushed inside the loop 6.

The narrowed zone 5 is positioned immediately after the waveguide 4 so that the repulsion of the second soliton towards the right hand side of the waveguide does not push it out through the waveguide 4. In this way the second soliton propagates far enough from the loop 8 to be attracted from it, while the first soliton is pushed inside loop 6 by the repulsive action between the two solitons.

6. Numerical simulation of the device

The designed device has been numerically simulated using a FD-BPM algorithm, to check the validity of the developed theory. The structure of the waveguides that compose the device are shown in Fig. 3(a).

We do not consider the left side of the loop waveguides since the most significant interaction effects take place in the merging point of the different waveguides, situated on the right-hand side of the structure.

The situations considered are the entrance of the first soliton inside the half-loop, the switching, operated from the first soliton with respect to the other solitons, and the exit of the first soliton from the loop waveguide to reach the output waveguides. The results are shown in Fig. 3. The numerical simulations confirm the correct behaviour of the designed device.

7. Operative considerations about the device

We have neglected, until this point, other secondary effects such as absorption and radiation, that unavoidably reduce the intensity of the beams until reaching the threshold under which they are no more trapped inside the loops.

The pulse that is mostly subjected to these effects is the first one, since it has to travel inside the loop a number of times that is equal to the number of pulses that compose the code.

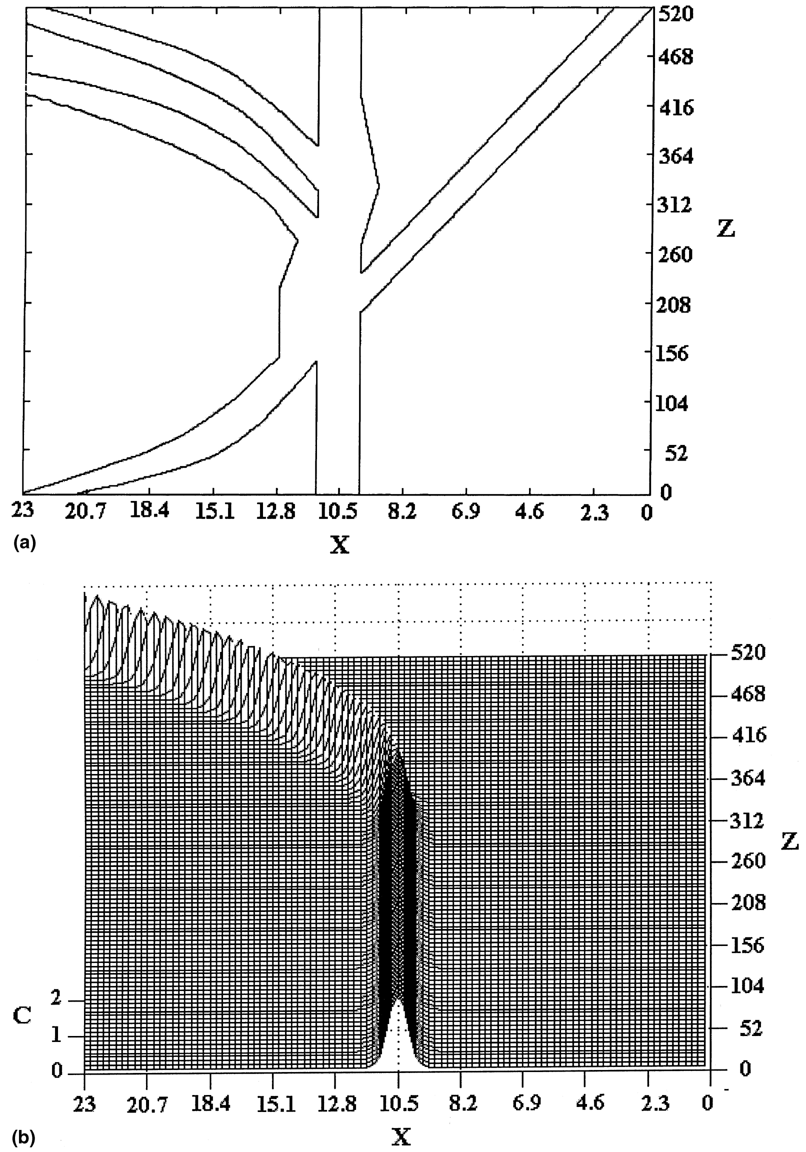

Fig. 3. Upper view of the significant structure, represented by the right hand side of the elementary loop cell, and numerical simulations. (a) Upper view of the structure, (b) Numerical simulation of the entrance of the first soliton inside the half-loop, (c) Numerical simulation of the switching operated from the first soliton with respect to the other solitons and (d) Numerical simulation of the exit of the first soliton from the loop waveguide to reach the output waveguides.

To compensate these effects it is necessary to increase the intensity of the soliton beams according to the influencing parameters, but the relative discussion is out of the scope of the paper.

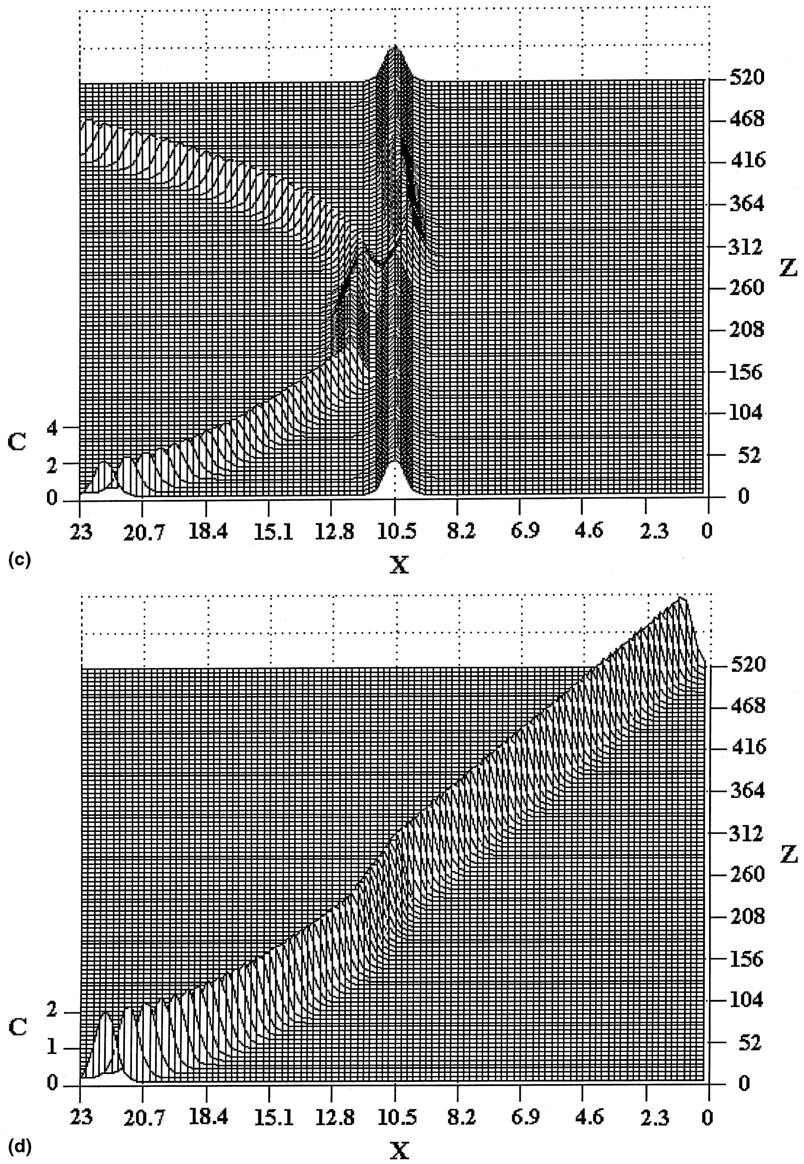

Fig. 3. (*Continued*)

The radiation does not take place if the paraxial approximation is respected, since the condition for the validity of NLSE, and therefore for the validity of the developed theory, are respected.

To see the influence of radiation on the performance of the device, non paraxial interactions have been numerically simulated, demonstrating how it already shows its effects in a FDTD algorithm applied to the NLSE. Further informations about radiation could be attained using a 2D FDTD algorithm but this is out of the scope of this paper that is to suggest the device and to verify its validity, restricting it to the validity of the NLSE.

In Fig. 4 the numerical simulations of induced radiating conditions, related to the switching operated from the first soliton with respect to the other solitons, are shown. The radiating conditions are induced increasing the inclination of left waveguide in the interaction zone so that the two soliton beams strongly collide, narrowing their profiles, generating strong index variations and sudden accelerations and not respecting locally the paraxial approximation.

In Fig. 4(a) a radiating condition is induced using a 10° collision angle between the two solitons. In this situation the two beams moderately deform they shape, increasing their amplitude and reducing their width, increasing further their transversal acceleration (Garzia *et al.* 1999): this situation induce unavoidably energy radiation with intensity reduction of both the solitons beams, implying a reduction of the number of times that the first soliton can be trapped inside the loop waveguide, that is directly related to its amplitude, as shown in Equation (3), and a reduction of the number of times that the other soliton can be trapped inside the loop of the following cell, letting anyway the device to work properly even if with a decrease of the performance.

In Fig. 4(b) a radiating condition is induced using a 15° collision angle between the two solitons. In this situation the two beams strongly deform their shape, increasing their amplitude and reducing their width: in this case most of the energy of the two solitons is lost by radiation with the results that the intensity of first soliton is below the threshold of the loop waveguide that is no more able to lock it in while the energy of the second soliton is too low that it can't interact with the following loop stage: the result is a total malfunctioning of the device due to energy radiation.

All these factors can be compensated increasing the intensity of the soliton but it can't anyway exceed four times the intensity of the base soliton to avoid the generation of second order soliton whose periodical change of profile alters the trajectories of the beams inside the waveguide. Further the more the intensity is closed to the intensity of the second order soliton and the more the profile aims at changing periodically: this change has to be considered to make the device work properly.

For this reason it is recommended to reduce all the lost factors more that increasing the intensity of the soliton beam.

The physical absorption can be reduced using a transparent material at the wavelength of the beam and using high quality mirrors. The absorption due to radiation can be reduced designing the device so that the interaction between solitons takes place gradually, respecting the restrictions imposed by the NLSE. In fact, even if the repulsion is weaker, increasing the total length

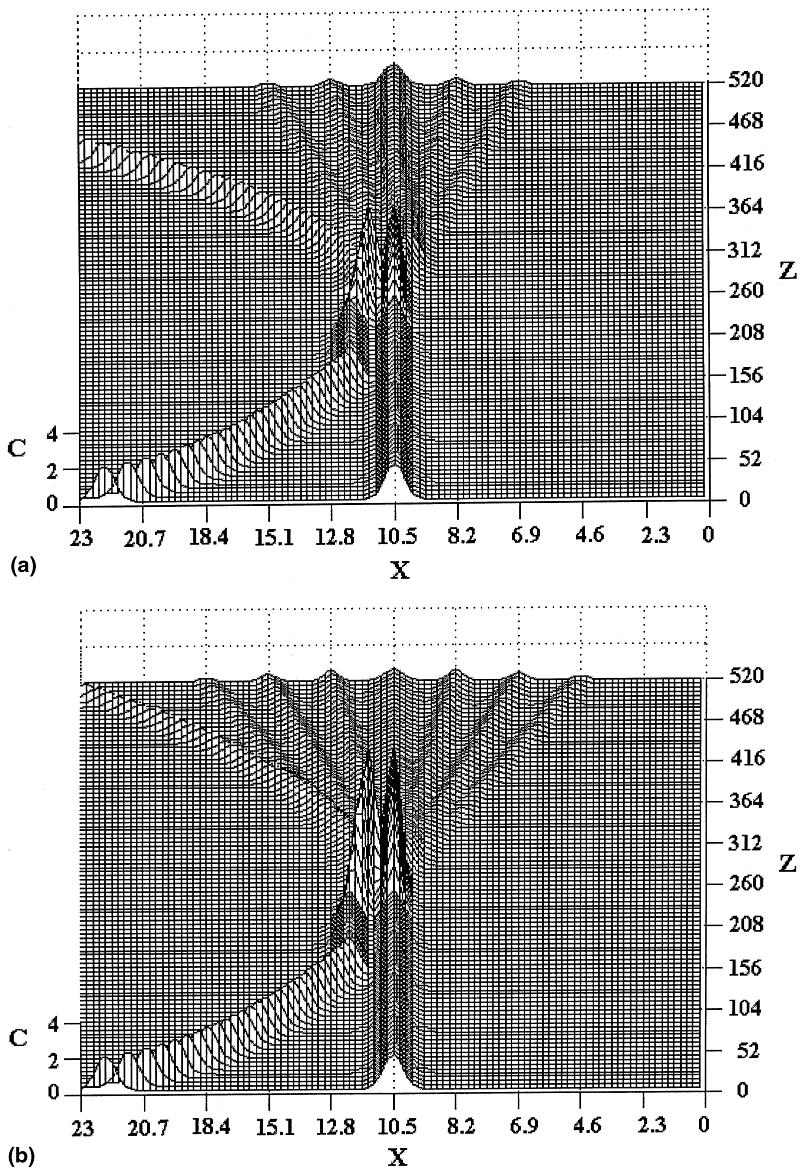

Fig. 4. Numerical simulation of the switching operated from the first soliton with respect to the other solitons in an induced non-paraxial condition, attained increasing the angle of collision: radiation takes place and the device does not work properly. (a) Angle of collision: 10° and (b) angle of collision: 15°.

of the device to attain a desired effect, the respect of the NLSE conditions does not allow energy lost, almost at this level of approximation: more intense interactions have demonstrated to radiate energy until inducing non-functioning conditions of the device.

8. Conclusions

We presented and designed an all-optical security coded key, based on the properties of soliton beams.

The switching properties have been studied in details, obtaining some useful criteria that help to design this kind of device.

The operative frequency is limited by the geometry of the device, by the response time of the nonlinear material and by the operative frequency of the source that generates the querying pulses.

The maximum number of bits that compose the code depends on the absorption properties of the device, whose reduction increases the number of bits that the device can handle.

References

Aceves, A.B., J.V. Moloney and A.C. Newell. *Opt. Lett.* **13** 1002, 1998.

Aceves, A.B., P. Varatharajah, A.C. Newell, E.M. Wright, G.I. Stegman, D.R. Heatley, J.V. Moloney and H. Adachihara. *J. Opt. Soc. Am. B* **7** 963, 1990.

Chen, H.W. and T. Liu. *Phys. Fluids* **21** 377, 1978.

Cow, S. *Sov. Phys. JETP* **55** 839, 1982.

Garzia, F., C. Sibilia and M. Bertolotti. *Opt. Comm.* **139** 193, 1997.

Garzia, F., C. Sibilia and M. Bertolotti. *Opt. Comm.* **152** 153, 1998.

Garzia, F., C. Sibilia and M. Bertolotti. *Opt. Comm.* **168** 277, 1999.

Garzia, F., C. Sibilia and M. Bertolotti. *Opt. Quantum Electron.* **32** 781, 2000.

Varatharajah, P., A.B. Aceves and J.V. Moloney. *Appl. Phys. Lett.* **54** 2631, 1989.